International Journal of Signal Processing, Image Processing and Pattern Recognition
Vol.8, No.6 (2015), pp.301-310
http://dx.doi.org/10.14257/ijsip.2015.8.6.32

A New Camera Calibration Method Based on Orientation Points in Digital Close-Range Industrial Photogrammetry

Huang Xuemei and Zhu Mingjian

School of mechanical engineering, Shandong University of Technology, Zibo255049, China
huangxuemei@sdut.edu.cn

Abstract

In order to solve the restriction of the two common calibration modes applied in digital close-range industrial photogrammetry, a new camera calibration method based on orientation points was proposed. Firstly, image sequences were obtained applying a calibration plate with five orientation points. The ellipse detection criteria were applied to eliminate the redundant information from images after pretreatment and all target points was determined as well. Then according to the special geometric relationship between orientation points, target points were matched exactly from object space to image space. Finally camera parameters were solved and optimized by the Gauss-Newton algorithm. In laboratory, the proposed theory was proved robust in Matlab2010 and could meet the measurement accuracy requirements.

Keywords: *cameral calibration; orientation points; automatic matching; Matlab2010*

1. Introduction

Digital close-range industry photogrammetry technology has advantages of high speed, non-destructive and non-contacting. Currently, it is widely applied in manufacturing, aerospace, urban planning, etc. [1-3].As one of the key steps of photogrammetry technology, camera calibration directly affects the final measurement results [4, 5]. Existing calibration methods (such as Zhang Zhengyou calibration method) mainly based on the checkerboard mode [6, 7]. This mode is sensitive to the image blur and noise because of its natural limitations. Usually calibrations with checkerboard mode require higher quality image to ensure the extracting accuracy for corners [8-11]. Compared to the checkerboard mode, calibration modes based on circular point's plate (all points have the same size, for convenient, circular calibration mode was called in this paper.) require lower image quality relatively. However, if multiple images needed to be calibrated in this mode, it would consume a long time and maybe cause mismatch [12, 13].

Based on problems mentioned above, a camera calibration method based on orientation points was proposed. In the premise of recognizing and matching five orientation points, other target points were matched automatically from object space to image space. Then the camera parameters could be computed and then optimized. In laboratory, a group of pictures was shot to verify the calibration method in this paper. The result showed the method was robust and could satisfy the accurate requirement of industrial measuring.

2. A Camera Calibration Method Based on Orientation points

A new calibration plate was designed based on the orientation points, as shown in Figure1. The coordinate origin O located in the bottom left of the calibration plate. Columns of target points along the X-axis positive direction were 11, and rows along the Y-axis positive direction were 9. The total number of target points was 99.

ISSN: 2005-4254 IJSIP

There were five asymmetric distribution big points (called orientation points) in calibration plate, and their diameter was significantly larger than others'. The labels of orientation points were 1 to 5(see Figure 1). The diameters were 20mm and 10mm for orientation points and remaining small target points, respectively (orientation points also belong to target points) . The horizontal and vertical distance of two target points were both 35mm.

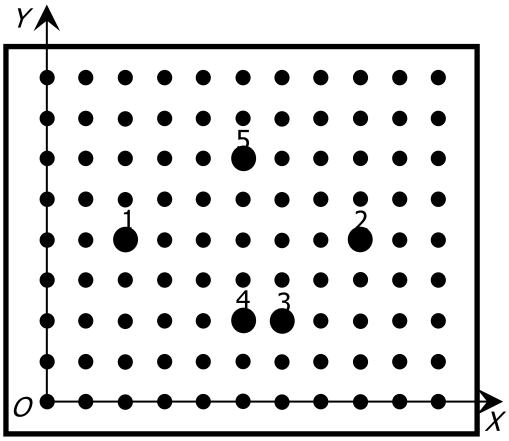

Figure 1. The Calibration Plate with Orientation Points

2.1. Acquiring and Preprocessing Images

The degree of image distortion was associated with the distortion coefficient and the focal length of camera. In order to reduce the influence of camera's distortion on the image quality and calibration results, pictures were shot without changing the focal length. The calibration plate should be kept parallel to the camera as far as possible, and images should be located in the center of the image plane. Each image was numbered and stored in the computer after shooting.

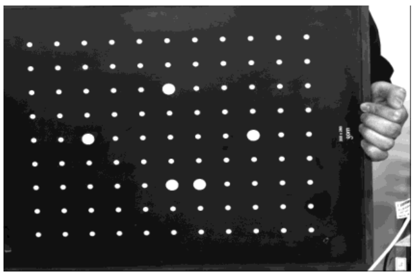

Figure 2. The Result of an Image after Pretreatment

In the process of camera calibration, the information of target points needed to retain, and redundant background information should be eliminated. So the threshold method was used for image binarization. Then the median filter was adopted for image noise-moving. The result of an image after pretreatment is shown in Figure 2.

2.2. Detecting the Target Points

When detecting target points, only contours 'information of points was needed for the further research. In this paper, Canny operator was used for edge detection in Matlab2010. The upper threshold was set for 0.3 and the lower threshold was 0.12. The red region in Figure 3(a) is enlarged and shown in Figure 3 (b).

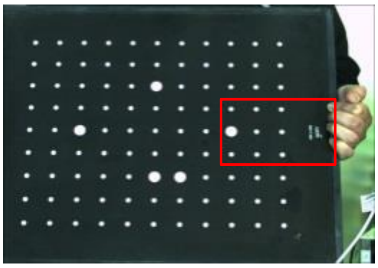

(a) The red area

(b) The enlarged area

Figure 3. Enlarged Image Area after Canny Edge Detection

As we can see clearly from Figure 3(b), in addition to contours' information of target points, there were other contours of impurities.

After the perspective transformation, shapes of target points changed from circle o ellipse. So ellipses detection criteria were designed to eliminate the redundant information from images. These criteria were summarized as follows:

(1) Straight line criterion. When the pixel's number of a contour was greater than eight along a certain direction, the contour was judged to be a straight line. Then the gray value of pixels set to zero.

(2) The length criterion. When a calibration plate designed strictly was shot, even the distortion and deflection occurred, contour sizes (circumferences) of orientation points N^1 and other target points N^2, always within a certain range, see (1).

$$\begin{cases} N^1_{min} < N^1 < N^1_{max} \\ N^2_{min} < N^2 < N^2_{max} \end{cases} \quad (1)$$

Where, N^1_{min} and N^1_{max} were thresholds range of circumferences for orientation points. N^2_{min} and N^2_{max} were thresholds range of circumferences for other target points.

(3) Shape criterion. In the same image, the distortion or zoom is also same. Closer target points were to the camera lens, bigger the image was. However, the ratio of major axis to minor axis for all ellipses was same. So the threshold P (P=2) could be set, impurities would be eliminated by the following equation.

$$\frac{a}{b} \leq P \quad (2)$$

In (2), a is the value of elliptic semi-major axis, and b is the value of semi-minor axis.

Figure 4 is the result of Figure 3 (b) after the processing steps mentioned above. Only ellipses of target points were retained. The redundant information was completely removed.

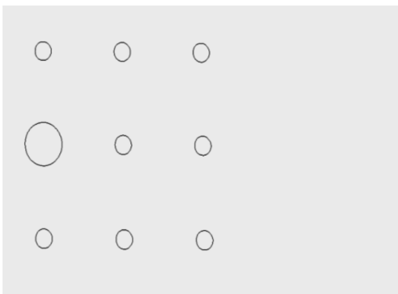

Figure 4. The Detecting Result of Partial Target Points

2.3. Automatic Matching Process

The aim of matching was to achieve the correspondence between image points and spatial points (target points). Orientation points were on the calibration plate in this paper, so the correspondent relations of five orientation points to five big ellipses could be determined firstly. Then orientation points were applied to determine the correspondent relation of other target points to small ellipses. Algorithms were described as follows:

(1) Firstly, determined correspondent relation of big ellipses in image to No.1 to No.5 orientation points. Five big ellipses could be distinguished easily according to their contour length. These big ellipses were marked F.

(2) Established the relationship of five big recognized ellipses to No. 1~5 orientation points, respectively. The process was as follows (see Figure1and Figure 5):

- Step 1, seek two ellipses that the distance between them was the longest, recorded F_1 and F_2 (marked any one of two ellipses F_1, the other was F_2). They must correspond to No. 1 or No. 2 orientation points. However, we did not know F_1 (F_2) correspond to which orientation point (No. 1 or No. 2).
- Step 2, Found two ellipses that the distance between them was the shortest, recorded F_3 and F_4. They must correspond to No. 3 or No. 4 orientation points. As before, we did not know F_3 (F_4) correspond to which orientation point (No. 3 or No. 4). Now only one ellipse was left, which was marked F_5. F_5 must correspond to No.5 orientation point.
- Step 3, connected centers of ellipses F_3 and F_4 to form line l_{34}。When l_{34} was rotated counter-clockwise, the first big ellipse it encountered must corresponded to No.2 orientation point and then this big ellipse was newly marked as F_2. The other big ellipse mentioned in step 1 must be F_1. Now F_1 and F_2 corresponded to No.1and No.2 orientation points, respectively.
- Step 4, computed center distances of F_1, F_3 and that of F_1, F_4. The big ellipse closer to F_1 newly marked as F_4, and the other is F_3. Now F_3 and F_4 corresponded to No.3 and No.4 orientation points, respectively.

(3) Determined correspondent relations between remaining image points and target points.

- Step 1, seek an image point(Q_1)that located the right side of the connection F_1 and F_4, and it should be the farthest point away from the connection F_1 and F_4. Q_1 corresponded to the target point on top right corner of calibration plate. Similarly , seek an image point(Q_2)that located the right side of the connection F_1 and F_5, and it should be the farthest point away from the connection F_1 and F_5. Q_2 corresponded to the target point on bottom right corner of calibration plate. Based on the same rule, we could matched target points on top left corner and bottom left corner of calibration plate to image points P_1, P_2, respectively.
- Step 2, From left to right, found all lines paralleled to line l_{P1P2}, and passed through all points on lines l_{P1Q1}, l_{P2Q2}, until the last line found was coincide with line l_{Q1Q2}.
- Step 3, all image points on lines found in step 2 were matched to target points on calibration plate sequentially.

The result of the final matching is shown in Figure 5. In Matlab2010, image points matched already to their space target points had been marked with red color. So the automatic matching was achieved finally.

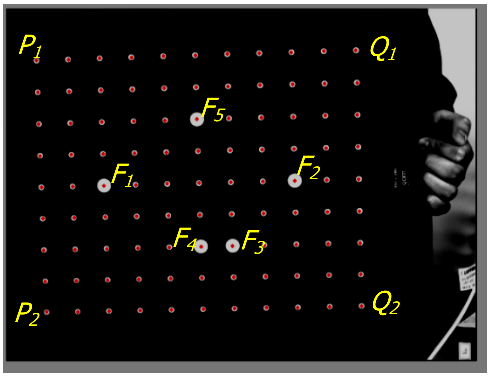

Figure 5. The Matching Result of the Target Points

2.4. Automatic Matching Process

After the completion of the matching, camera parameters could be obtained according to the relation between the world coordinate system and the image coordinate system, see (3).

$$\lambda\begin{bmatrix}x\\y\\1\end{bmatrix}=\begin{bmatrix}u\\v\\1\end{bmatrix}=K\begin{bmatrix}R & t\end{bmatrix}\begin{bmatrix}X_w\\Y_w\\0\\1\end{bmatrix}=K\begin{bmatrix}r_1 & r_2 & r_3 & t\end{bmatrix}\begin{bmatrix}X_w\\Y_w\\0\\1\end{bmatrix}=K\begin{bmatrix}r_1 & r_2 & t\end{bmatrix}\begin{bmatrix}X_w\\Y_w\\1\end{bmatrix} \quad (3)$$

Where, for a certain target point, (X_W, Y_W, Z_W) was its coordinate value of in world coordinate system, and in this paper, Z_W=0 for plane calibrated plate was applied. (x, y)was the coordinate value of the projection of (X_W, Y_W, Z_W)in image coordinate system, and λ was the scale factor. (u, v) was the coordinate value of the projection of the point in pixel coordinate system (pixel coordinate system was also located in image plane. However, its origin of coordinate was located in the top left corner). K was internal parameters of the camera, determined by the structure of camera. R and t were external parameters of the camera. R= [r_1 r_2 r_3] was the rotation matrix, and t was the translation vector. K, R and t were also called calibration parameters.

Eq. (3) could be transformed to (4).

$$K=\begin{bmatrix}\frac{1}{dx} & 0 & c_x\\0 & \frac{1}{dy} & c_y\\0 & 0 & 1\end{bmatrix}\begin{bmatrix}f & 0 & c_x & 0\\0 & f & c_y & 0\\0 & 0 & 1 & 0\end{bmatrix}=\begin{bmatrix}f_x & 0 & c_x & 0\\0 & f_y & c_y & 0\\0 & 0 & 1 & 0\end{bmatrix} \quad (4)$$

Where, dx, dy was the actual size of a pixel in x direction and y direction of image plane. f was the camera focal length. f_x and f_y were projection size of focal length in x direction and y direction of image plane.(c_x, c_y) were the coordinate value of the center of camera in image coordinate system.

For all target points and their correspondent image points, according to the coordinate values of world coordinate system and image coordinate system, internal parameters of the camera and external parameters for every image could be obtained. For the limited space, the author would not describe in detail.

3. Optimization of Camera Parameters

Due to various distortions, etc., camera parameters obtained were only rough values. In order to improve their accuracy and conform to the requirements of camera calibration, the optimal camera parameters could be required further. In this paper, an optimal method was found to make following (5) minimizing.

$$\sum_{p=1}^{n}\sum_{q=1}^{m}\left\| m_{pq} - m^{'}\left(K, k_1, k_2, R_p, t_p, M_q\right)\right\|^2 \tag{5}$$

Where, m_{pq} was coordinate value of point q on image p in the pixel coordinate system. M_q was coordinate value of point q on image p in the world coordinate system. After rough values of internal parameters was obtained, we could calculate the re-projected value $m'(K, k_1, k_2, R, t, M_q)$ of m_{pq} in pixel coordinate system. k_1, k_2 was the distortion factor of the camera.

Solving (5) involved the complex nonlinear least squares problem which generally does not have closed-form solutions. Usually this problem solved by LM (Levenberg-Marquardt) iteration algorithm. However, there are some problems in practical application, such as the damping factor value is difficult to determine, converge slowly et al. Gauss - Newton method has good convergence, therefore Gauss - Newton method was combined LM algorithm to obtain the minimum value of (5). Solving process was as follows:

(1) Firstly, all calibration parameters in (5) were represented by a vector X, then (5) could be expressed as:

$$\sum_{i=1}^{s}\left\| m_i - m^{'}(X)\right\|^2 = \sum_{i=1}^{s}\sigma_i^2(X) \tag{6}$$

Where, s represented the number of target points in all images, namely $p\times q$. $\sigma_i(X)$ was the re-projection error of the target point ith. $X^{(k)}$ was obtained after k iterations operation to X. $\sigma i(X)$ could be linearized by applying Taylor series expansion at $X^{(k)}$.

(2) Second, $X^{(1)}$ (rough values of camera parameters) was set as the initial value of X. Maximum allowable error ε judging the iteration convergent and the maximum number of iterations Max were both set. Then from number 1, all vectors of objective function could be obtained after k iterations computing.

$$\sigma(\mathrm{X})^{(k)} = \begin{bmatrix} \sigma_1(X^{(k)}) \\ \sigma_2(X^{(k)}) \\ \vdots \\ \sigma_i(X^{(k)}) \end{bmatrix} \tag{7}$$

First order partial derivatives of calibration parameters could be solved by (7), see following equation.

$$\alpha_{ij} = \frac{\partial\sigma_i\left(X^{(k)}\right)}{\partial X^j}(i = 1, 2 \ldots s; j = 1, 2 \ldots n) \tag{8}$$

Eq. (8) could be expressed by a matrix.

$$\mathrm{A}_k = \begin{bmatrix} \frac{\partial\sigma_1(X^{(k)})}{\partial X^1} & \cdots & \frac{\partial\sigma_1(X^{(k)})}{\partial X^n} \\ \vdots & \cdots & \vdots \\ \frac{\partial\sigma_s(X^{(k)})}{\partial X^1} & \cdots & \frac{\partial\sigma_s(X^{(k)})}{\partial X^n} \end{bmatrix} \tag{9}$$

Then, linear equations $\mathrm{A}_k d = -\mathrm{A}_k^{\mathrm{T}}\sigma_{\mathrm{i}}(X^{(k)})$ was used to solve modifying factor d.

Finally, make $X^{(k+1)} = X^{(k)} + d$. Maximum allowable error ε and the maximum number of iterations Max was applied to judge: If $\| X^{(k+1)} - X^{(k)} \| \leq \varepsilon$ or $k \geq Max$, then stop counting, and set $X = X^{(k+1)}$; Otherwise, make $k = k + 1$, start again.

The camera parameters could be improved more precisely through the above iteration process; thereby the accuracy of the measuring results was further improved.

4. Experimental Verification and Analyzing

The proposed theory of camera calibration was carried out by programming in Matlab2010 environment. German Basler ACA1600-20gm camera and Japanese computar industrial lenses were applied for image acquisition, as shown in Figure 6. The resolution of camera is 1626 × 1236; the lens focal length is 8mm.Total nine pictures of calibration plate were taken from different angles as experiment data by hand-held camera mentioned above. Preprocessed images are shown in Figure 7.

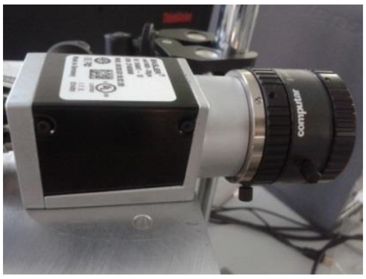

Figure 6. The Camera Applied in Experiment

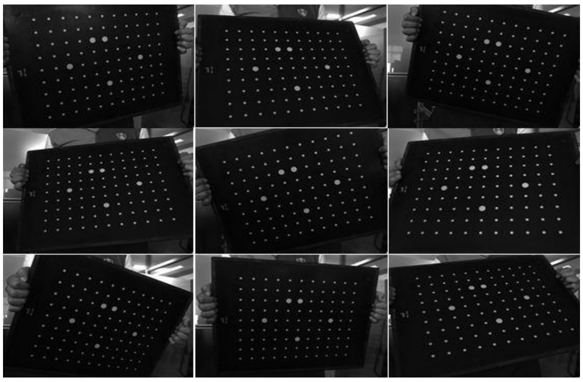

Figure 7. Images after Preprocessing

ε was set for $10^{-9}$and *Max* = 20. Then internal camera parameters and distortion factor obtained in this paper were as follows:

$$K = \begin{bmatrix} 1904.2321 & 0.0000 & 838.0323 & 0.0000 \\ 0.0000 & 1905.1287 & 614.0071 & 0.0000 \\ 0.0000 & 0.0000 & 1.0000 & 0.0000 \end{bmatrix}$$

Distortion coefficient k_1=-0.084，k_2=0.14313.

To show the robustness of new calibration method, camera parameter *K'* was also solved applying checkerboard calibration method.

$$K' = \begin{bmatrix} 1947.5246 & 0.0000 & 819.1256 & 0.0000 \\ 0.0000 & 1948.1482 & 598.0128 & 0.0000 \\ 0.0000 & 0.0000 & 1.0000 & 0.0000 \end{bmatrix}$$

The results of comparison of *K* to *K'* were shown in Table 1. As we can see from Table 1, relative errors were within ± 2.5% for values of the focal length and the center of camera in new method compared to those in checkerboard method. Errors were in a small range, which verified the robustness of the calibration method put forward in this paper.

The distribution degree of the re-projection error can reflect the accuracy of camera calibration result. More intensive the distribution was, more accurately calibration parameters were solved previously. So circular calibration mode and new calibration mode in this paper were both adopted to calibrate the camera, and then results were re-projected. Errors of re-projection for nine pictures were shown in Figure 8(a) and Figure 8(b), respectively.

Table 1. The Comparison of the Camera Parameters

parameters	checkerboard calibration method	New calibration method	relative error
f_x	1947.5246	1904.2321	-2.2230%
f_y	1948.1482	1905.1287	-2.2208%
c_x	819.1256	838.0323	2.3082%
c_y	598.0128	614.0071	2.6746%

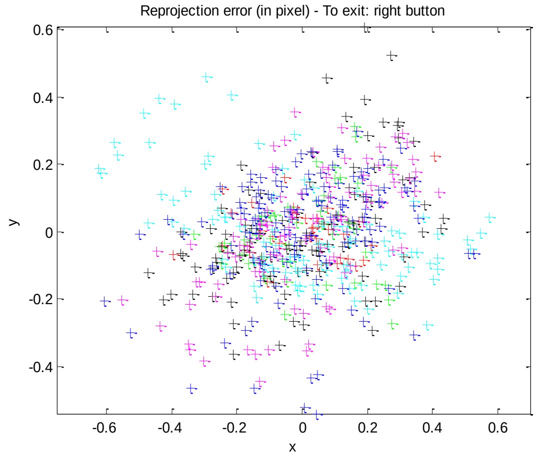

(a) The re-projection error based on circular calibration

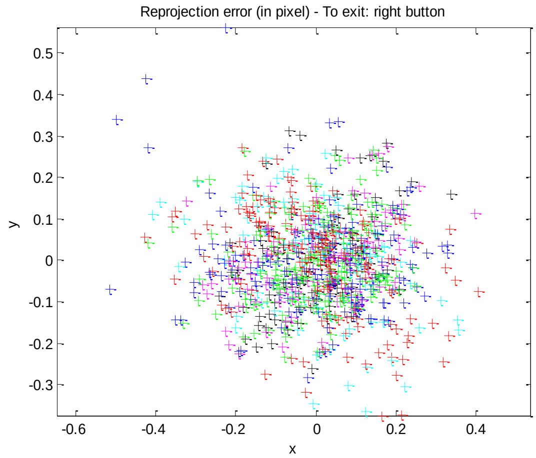

(b) The re-projection error based on calibration mode in this paper

Figure 8. The Re-projection Error Distribution Map

In Figure 8(a), the error in the Y-direction was about 0.6 pixels, and the error in the X-direction was about 0.6 pixels. In Figure 8(b), the error in the Y-direction was about 0.3 pixels and that in the X-direction was only about 0.4 pixels. And the distribution of re-projection error in Figure (8) b was more intensive. These results proved that the camera calibration accuracy based on new calibration mode was better than that based on circular calibration mode in the case of applying the same picture quality.

Figure 9 showed the comparison of matching time spent in new calibration mode and circular calibration mode, respectively. The new calibration mode took about 40s, less than 70s spent in circular calibration mode. This result verified that the calibration method proposed in this paper could improve the efficiency of calibration.

5. Conclusion

A camera calibration method based on orientation points was proposed in this paper, and its experimental verification was carried out in Matlab2010, the following conclusions can be drawn:

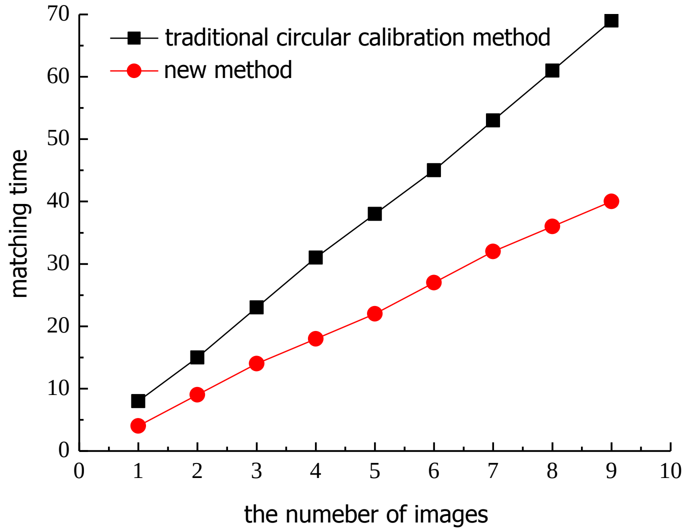

Figure 9. Time Consuming Comparison Chart for Target Points Matching

(1) Compared to checker-board calibration method, the calibration mode put forward in this paper also had robust performance, and could satisfy the accuracy demanding of industrial photogrammetry.

(2) Re-projection errors of nine pictures applying two different calibration modes were comparatively analyzed. The calculated result showed that the accuracy of the camera parameters obtained in new calibration mode is higher than that obtained in circular calibration mode.

(3) The matching time for target points shown that the calibration method in this paper had higher efficiency compared to circular calibration method.

Acknowledgements

This work is sponsored by Shandong provincial Natural Science Foundation, China (No. ZR2012EEL11).

References

[1] M. Ahmed, C. T. Haas, and R. Haas, “Can. J. Civ. Eng.”, vol. 39, 1062 **(2012).**
[2] M. Z. Chen, “Appl. Mech. Mater.”, vol. 170, 2979 **(2012).**
[3] R. Liu, Y. F. Zhu, Y. Luo and X. T. Liu, “Proc. - Int. Forum Inf. Technol. Appl.”, IFITA., vol. 1, no. 536 **(2009).**
[4] D. Q. Tao, Z. Y. Yin, S. X. Liu and L. J. Wang, “Adv. Mater. Res.”, vol. 271, no. 489, **(2011).**
[5] H. C. Yang, K. Z. Deng, S. B. Zhang, G.L. Guo and M. Zhou, “J. China Univ. Min. Technol.”, vol. 16, no. 119, **(2006).**
[6] Z. Y. Zhang, “IEEE Transaction on Patter Analysis and Machine Intelligence”, vol. 22, no. 1330**, (2000).**
[7] S. D. Ma and Z. Y. Zhang, “Computer vision: The calculation theory and algorithm”, Science press, Beijing **(1998).**

[8] D. Y. Ge and X. F. Yao, "Journal of Optoelectronics Laser", vol. 21, no. 1720, **(2010).**
[9] S. Cai, Z. J. Zhao, L. X. Huang and Y. C. Liu, "Machine Vision and Applications", vol. 24, no. 513, **(2013).**
[10] Q. Ji and Y. M. Zhang, "Systems, Man and Cybernetics", Part A: System and Humans", vol. 31, 120, **(2001).**
[11] F. Espuny, "Journal of Mathematical Imaging and Vision", vol. 27, no. 81**, (2007).**
[12] J. Sun and H. B. Gu, "World Academy of Science, Engineering and Technology", vol. 60, no. 627, **(2011).**
[13] X. F. Yang, Y. M. Huang, F. Gao, X. G. Yang and X. Z. Han, "Chinese Journal of Scientific Instrument", vol. 32, no. 1109**, (2011).**

Authors

Huang Xuemei, She received the BS degree in Mechanical Engineering from Shandong University of Technology, China, in 1997, and her MS and PhD degrees in Mechanical Engineering from Shandong University and Shanghai Jiaotong University, China, in 2001and 2004, respectively. She is an associate professor in College of Mechanical Engineering, Shandong University of Technology. Currently she is interested in digital design and manufacturing.

Zhu Mingjian, She received the BS degree in Shandong University of Technology, Shandong, China, in 2012. Now she is a graduate student in College of Mechanical Engineering, Shandong University of Technology, China. Presently she is interested in digital design and manufacturing.